ISSN: 0067-2904

Influence of Magnetic Field on Silver Nanoparticles Synthesized by Laser Ablation

Zahraa Marid Abbas*, Qusay Adnan Abbas
Department of Physics , College of Science , University of Baghdad, Baghdad, Iraq.

Received: 11/7/ 2019 Accepted: 28/ 8/2019

Abstract

Laser ablation of a silver target immersed in distilled water using Nd:YAG laser with a fundamental wavelength of 1064nm was carried out to fabricate silver nanoparticles (Ag NPs) with different laser energy in the presence and absence of magnetic field. UV-Visible spectrum showed that the nanoparticles are almost spherical in shape. The number of Ag NPs increased by increasing laser energy while their particle size was reduced by increasing laser energy without magnetic field. In the presence of magnetic field, the size of Ag NPs increased slightly by increasing laser energy. According to AFM results, the presence of magnetic field did not affect the average diameter of Ag NPs. The presence of a magnetic field causes a change in grain size of Ag NPs with increasing laser energy. While XRD data illustrated that the magnetic field causes an increase in the crystallite size of Ag NPs.

Keywords: Laser ablation, Surface Plasmon Resonance (SPR), Silver nanoparticles, Magnetic Field.

تأثير المجال المغناطيسي على جسيمات الفضة النانوية المحضرة بالاستئصال بالليزر

زهراء مارد عباس*، قصي عدنان عباس
قسم الفيزياء، كلية العلوم، جامعة بغداد، بغداد، العراق

الخلاصه

تم إجراء التذرية بالليزر لهدف من الفضة مغمورة في الماء المقطر باستخدام ليزر ND:YAG ذو طول موجي 1064 nm لتصنيع جسيمات الفضة النانوية وعند طاقة الليزر المختلفة وفي حالة وجود وغياب المجال المغناطيسي. تم فحص ومقارنة خصائص الجسيمات النانوية الفضية في الماء المقطر.حيث أظهر الطيف المرئي فوق البنفسجي شكلًا كرويًا تقريبًا ، وان عدد Ag NPs المضرة تزداد بزيادة طاقة الليزر وان حجم Ag NPs يقل بزيادة طاقة الليزرفي حالة عدم وجود مجال مغناطيسي. اما في حالة تلسيط مجال مغناطيسي فأن حجم Ag NPs ينمو قليلاً عن طريق زيادة طاقة الليزر. كذلك بينت النتائج ، حدوث زيادة في عدد Ag NPs المضرة في حالة وجود مجال مغناطيسي في نفس طاقة الليزر. وفقا لنتائج AFM ، فإن وجود مجال مغناطيسي لم يؤثر على متوسط قطر .AgNPs المحضرة انما يتسبب وجود مجال مغناطيسي في تغيير حجم جسيمة AgNPs مع زيادة طاقة الليزر. بينما أوضحت بيانات XRD أن المجال المغناطيسي يؤدي إلى زيادة حجم البلوري ل AgNPs .

1. Introduction

In liquids, pulse laser ablation (PLA) of solids is a technology for generation of nano-particles [1]. This technique has been studied in recent years because of the present numerous potential in laser

*Email: zahraamarid@yahoo.com.

material micro-processing, including nanomaterials and nanostructures synthesis [2]. Laser-assisted formation of nanoparticles is the result of a laser beam bump on a target and the subsequent removal of material from the target surface, promoted by the liquid enclosed by vapor. At sufficiently high laser fluence, the target surface layer suffers melting. The medium around the target, which is liquid under normal conditions, departs to the overheated gaseous state. Compared to other methods, typically chemical methods, PLA in liquid is a simple and "green" technical method that normally acts in water or organic liquids under ambient conditions [2-4].

Metal nanoparticles are more attractive because of their physical and chemical properties which depend on their size. Formation of metal nanoparticles by laser ablation of solids in a liquid environment is an reciprocal method to the well-known chemical methods and is characterized by relatively simple experimental setup. In comparison with the chemical methods, laser ablation generates metal nanoparticles while the surface is not contaminated with residual ions originating from the recants. It is well known that the optical absorption spectra of metal nanoparticles are dominated by surface-plasmon resonance (SPR), with the shift to longer wavelengths with increasing particle size [5]. Noble metals such as silver nanoparticles (NPs) have received immense attention due to their excellent electrical, optical, physical, chemical and magnetic properties [6-8]. The localized surface plasmon resonance (LSPR) is another characteristic of silver nanoparticles that is the effect of the collective oscillation of the excited conduction electrons by the incident electromagnetic radiation.

When the light interplays with spherical Ag nanoparticles of a few nanometers, the incident electromagnetic field radiation shifts the conduction electrons from their restoring force, resulting in a collective oscillation of the electrons at a characteristic frequency. The resonance of LSP occurs near 400nm for Ag NPs. At the same time, the oscillation of the electrons produces a polarization in the opposite sense in the surrounding medium of the generated particle. This polarization abates the strength of the restoring force over the nanoparticle, leading to a shift in LSPR depending of the surroundings characteristic [7]. Noble metal nanoparticles have been very attractive for biochemical, biophysical and biotechnological applications due to their extraordinary physical properties, particularly due to their sharp plasmon absorption peak in the visible region. Another important benefit of Ag NPs synthesized by pulsed laser ablation in liquid (PLAL) is its chemical stability for a duration of months. Additionally, Ag NPs typically demonstrate surface enhanced Raman scattering (SERS) in the visible region, where they may cause a severe increase in various optical cross-sections, along with laser deposition, chemical reduction, photo reduction, electrochemical reduction,...etc [9].

The synthesis methods, stability, and characteristics of Ag NPs have become the subject of many researches in recent years. Currently, nanomaterials based on Ag NPs are applied in chemical, optical, electronic, and textile industries, as well as in pharmaceuticals, cosmetology, medicine, food production and packing. They play an important role as substrates for the production of catalytic materials, sensors, conductors, detergents and antimicrobial coatings [10-12].

The aim of this work is to study the influence of magnetic field on the characteristics of Ag NPs prepared by laser ablation at different pulse laser energy.

2. Experimental part

Ag NPs were prepared by laser ablation of high purity silver (99.999%) circular target with distilled water in the presence and absence of magnetic field (Figure-1). Q-switched Nd:YAG laser with fundamental wavelength of 1064 nm, pulse duration of 10 ns and 6 Hz repetition rate at different pulse energy (500, 600 and 700 mJ) was used for the ablation of the Ag target which was rotating through the distilled water. Silver circular bulk was placed at the bottom of a water container, with its surface being at the focal point of a 100 mm convex lens. Height of water on the silver target was 10 mm. The volume of the water in the ablation container was 3 ml and the silver target was ablated with a number of shots of 500 pulses at different laser pulse energies. A magnetic field of 4.4 mT was applied using a permanent magnet.

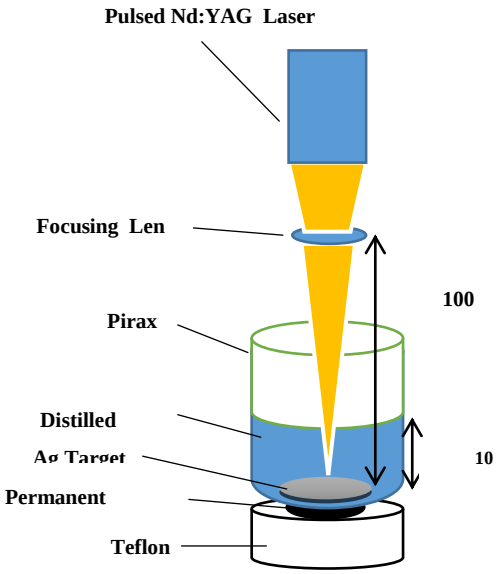

Figure 1-Schematic diagram of eperimental setup for laser ablation of silver disc target immersed in distilled water.

3. Characterization of the Synthesized Silver Nanoparticles

Several experimental methods are available to characterize the synthesized AgNPs. The localized surface plasmon resonance of silver nanoparticles was characterized by using UV–Vis spectrophotometer [Shimadzu model) over a wavelength range of 190-1100 nm. The size and morphology of AgNPs were characterized by AFM (Angstrom advanced SPM-A 3000 model) and the presence of elemental silver was confirmed through X-ray diffraction (SHIMADZ XRD 600C) analysis with Cu-kα x-ray tube (λ=1.5418A^0, V=40 kV, I= 30 mA). The interaction between distilled water and AgNPs was analyzed by Fourier transforms infrared spectroscopy (FTIR) (SHIMADZU) that provides a record of absorption of electromagnetic radiation by a sample in the range of wavenumber of 400-4000 cm^{-1}.

4. Results and Discussion

4.1 Influence of Pulse Energy on the Ag Nanoparticles Solution

Figure-2 shows the photos of the Ag NPs prepared in distilled water in the presence and absence of magnetic field at different pulse energies. One can observe that the color of Ag NPs solution in distilled water changes from light yellow to yellow with increasing laser energy with the magnetic field. The color of the Ag NPs solution changed gradually to brown in the absence of magnetic field. Color changes that were observed with increasing laser energy can be due to the amount and sizes of nanoparticles [13]. By decreasing the size of Ag NPs, their color changed from yellow to brown. If we compare the samples in the presence and absence of magnetic field, we can conclude that the amount of Ag NPs increased without magnetic field, but the size of Ag NPs was smaller.

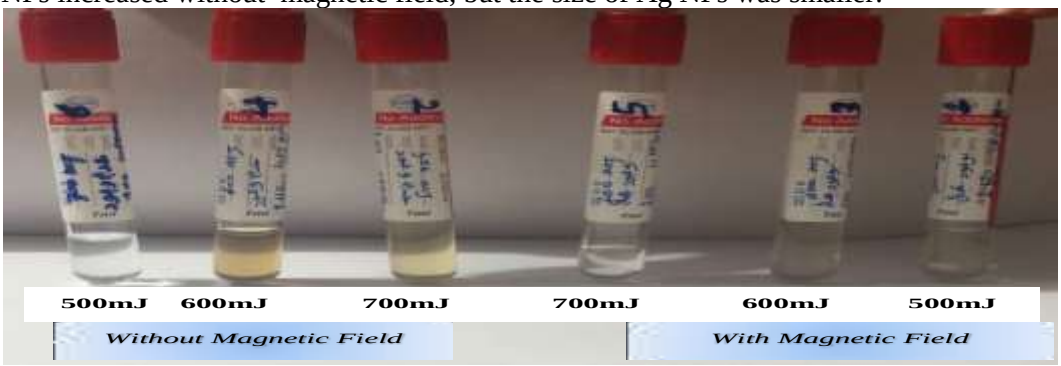

Figure 2-Ag nanoparticles samples in distilled water in the presence and absence of magnetic field.

4.2 X-ray Diffraction

The XRD analysis was employed to determine the phase distribution and crystallinity of the synthesized nanoparticles. Typical XRD patterns of the dried powder of the prepared Ag- NPs is shown in Figure-3.

The peaks appearing in Figure-3 are namely those at (200) and (220) and are due to the Ag cubic structure (JCPDS data file No.4-0783), which also indicates a high purity of the prepared Ag NPs. The sharpness of the reflection peaks provides a clear evidence for the enhanced crystallinity of the Ag nanostructures. The mean crystallite sizes of Ag-NPs were estimated from Debye- Scherer formula [6,8]:

$$D = \frac{0.89\lambda}{\beta \cos\theta} \quad (1)$$

where D is the mean crystallite size, λ is the wavelength of the X-ray radiation, θ is the diffraction angle, and β is the full width at half maximum (FWHM). The structural parameters of Ag-NPs are shown in Table-1.

From the data indicated in Table-1, it is clear that the average crystallite size achieved without magnetic field is equal to 32.26 nm. While when the magnetic field was applied, the average crystallite size became 39.93nm.

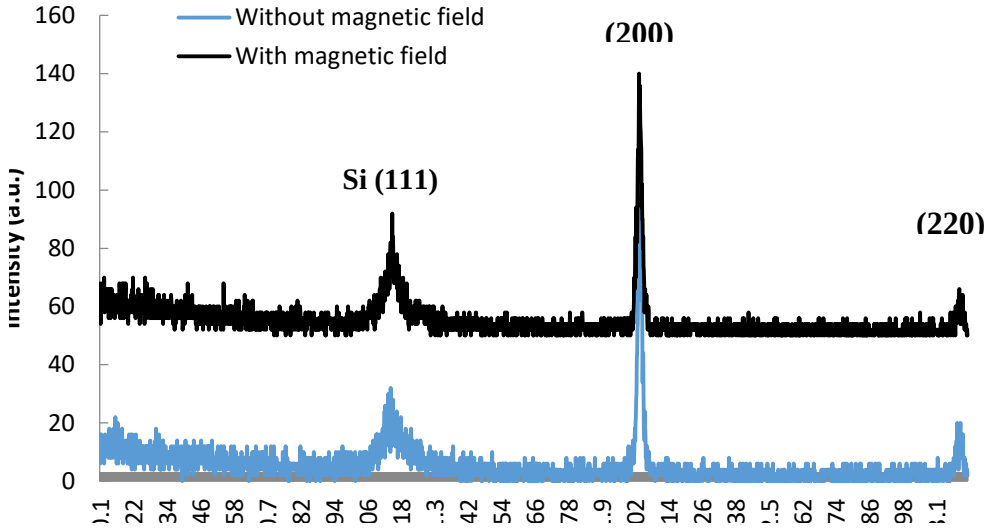

Figure 3-X-ray diffraction pattern of Ag nanoparticles in the presence and absence of magnetic field.

Figure 3-X-ray diffraction pattern of Ag nanoparticles in the presence and absence of magnetic field.

Without Magnetic Field				
2θ (deg)	**(hkl)**	**d-spacing (A^0)**	**FWHM (deg)**	**Crystallite Size (nm)**
44.2995	(200)	2.04615	0.31	27.357
64.5879	(220)	1.4418	0.25	37.169
With Magnetic Field				
44.213	(200)	2.04688	0.25360	33.432
64.4629	(220)	1.44429	0.20	46.43

4.3 UV-VISIBLE Analysis

The UV-Visible spectrum of Ag solution that prepared at different pulse laser energies in the presence and absence of the magnetic field is plotted in Figure- 4. The UV-Visible spectrum in Figure-4A shows an SPR peak of Ag nanoparticles at 410, 399 and 404 nm at pulse laser energy that ranged between 500, 600 and 700 mJ, respectively. The appearance of this SPR peak in this range is due to

Mie scattering [14]. The UV-Visible spectrometer is the effective method to evaluate the size and shape of nanoparticles in water. It has been reported that the spherical shaped AgNPs have an absorbed SPR band at around 400-420 nm [13,14]. This result indicated that the synthesized Ag nanoparticle has a spherical shape. In addition, the results show that the SPR peak intensity was increased with increasing laser energy. The increase in SPR intensity was associated with an increase in the number of the formed AgNPs [15]. Therefore, this result indicated that the number of the formed Ag nanoparticles increased with the increase in laser energy. The results also showed that the SPR peak was shifted to shorter wavelength (blue shifted) with increasing laser energy, which indicates the formation Ag NPs with larger size. In addition, the absorption curve gives an evidence that laser energy affected the LSPR position, indicating that there was no symmetric nanostructures produced for all fabrication conditions.

Figure -4B demonstrates the UV-Visible spectrum of Ag nanoparticle solution prepared at different laser energies in the presence of a magnetic field. The spectrum shows that the SPR Peak appeared at 407, 400 and 403 nm when the pulse laser energy was 500, 600 and 700 mJ, respectively. The SPR peak was shifted toward a shorter wavelength with increasing laser energy. This shift implies that the nanoparticle size increased with increasing laser energy, according to Mie theory [13]. The comparison between Figures- 4A and 4 B shows that the SPR peak was slightly devoid toward shorter wavelength when the magnetic field was applied. This result indicated the fact that the Ag nanoparticle size slightly increases in the presence of a magnetic field. This behavior can be explained by the fact that the silver material is diamagnetic material, so that silver atoms have no unpaired electrons, which results in a zero net magnetic moment. Therefore, sliver material displays a very weak response against the applied magnetic field due to realignment of the electron orbits when a magnetic field is applied. They do not retain magnetic moment when the magnetic field is removed [15]. The intensity of SPR peak was increased in the presence of magnetic field. This means that the number of Ag nanoparticles increases in the presence of magnetic field.

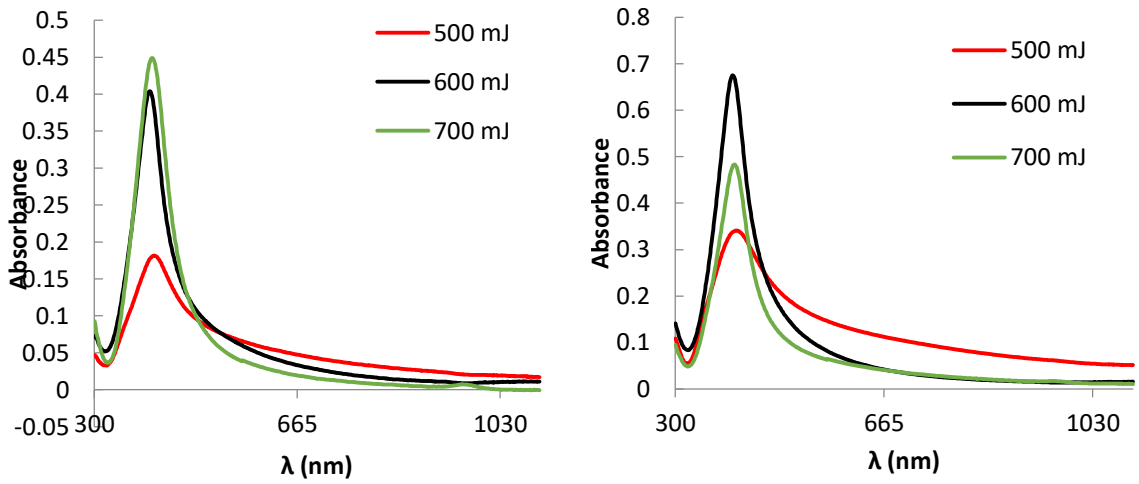

Figure 4-UV-Visible spectrum of Ag nanoparticle in distilled water synthesized at different pulse laser energy; **A)** without magnetic field and **B)** with magnetic field.

4.4 AFM analysis

The morphology of the synthesized Ag NPs was analyzed by atomic force microscope (AFM) at different laser energies in the presence and absence of magnetic field. This technique can provide a visualization of individual particles and groups of particles and in three dimensions, unlike other microscopy techniques. Figures 5 and 6 show the AFM images of AgNPs synthesized at different pulse laser energies in the absence and presence of magnetic field, respectively. One can observe from Figure- 5 that the average depth of AgNPs was 18.51, 2.23 and 6.08 nm which corresponds to pulse energy of 500 mJ, 600 mJ and 700 mJ, respectively. On the other hand, when the magnetic field was present, the results in Figure- 6 show that the AgNP depth was changed to become 7.72, 5.54 and 24.72 nm, corresponding to laser energy of 500, 600 and 700 mJ, respectively. The average diameter and roughness of Ag NP in the presence and absence of magnetic field are tabulated in Table- 2. The

table indicates that the average diameter of the AgNPs was reduced and then increased with the increasing of pulse laser energy values, with and without magnetic field respectively. The increase of the average diameter can be explained by the fact that, with increasing laser energy, the ablation process is accompanied by melting the Ag target surface, with less evaporation and NP auto-absorption of laser photons. This absorption leads to the formation of smaller particles as a result of fragmentation of larger ones [11]. While the increase in the average diameter of Ag NP with increasing laser energy from 600 mJ to 700 mJ may be attributed to the rapidly decreased ablation efficiency with increasing the laser pulse energy. This behavior was ascribed to the occurrence of auto-absorption processes leading to fragmentation of larger particles and consequently decreasing the average diameter of AgNPs [11].

Without Magnetic Field		
Laser Energy (mJ)	**Average Diameter (nm)**	**Roughness Average (nm)**
500	79.08	4.16
600	55.68	0.523
700	65.26	0.509
With Magnetic Field		
500	73.54	1.72
600	63.61	1.38
700	68.11	6.42

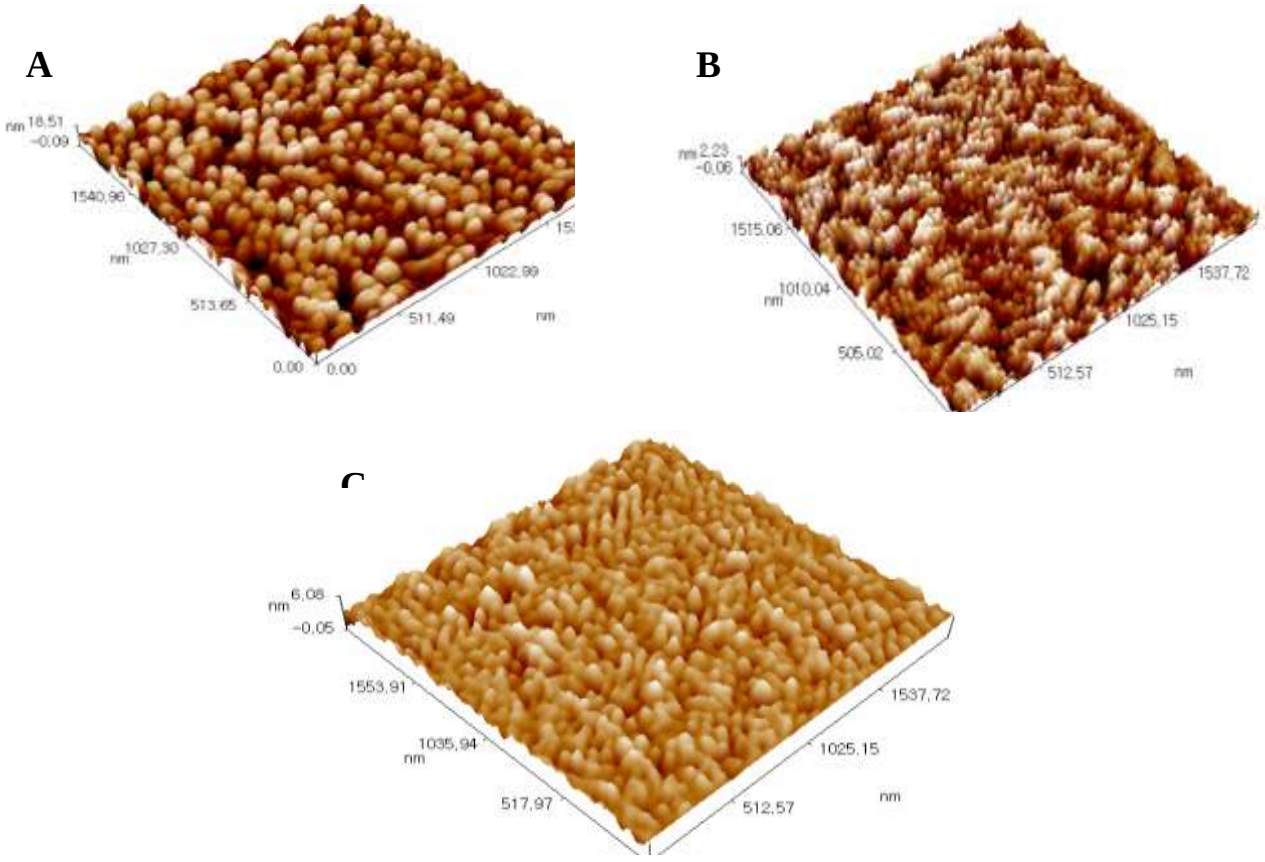

Figure 5-AFM images of Ag nanoparticles prepared at different pulse laser energies A) 500Mj, B) 600mJ and c) 700mJ without magnetic field.

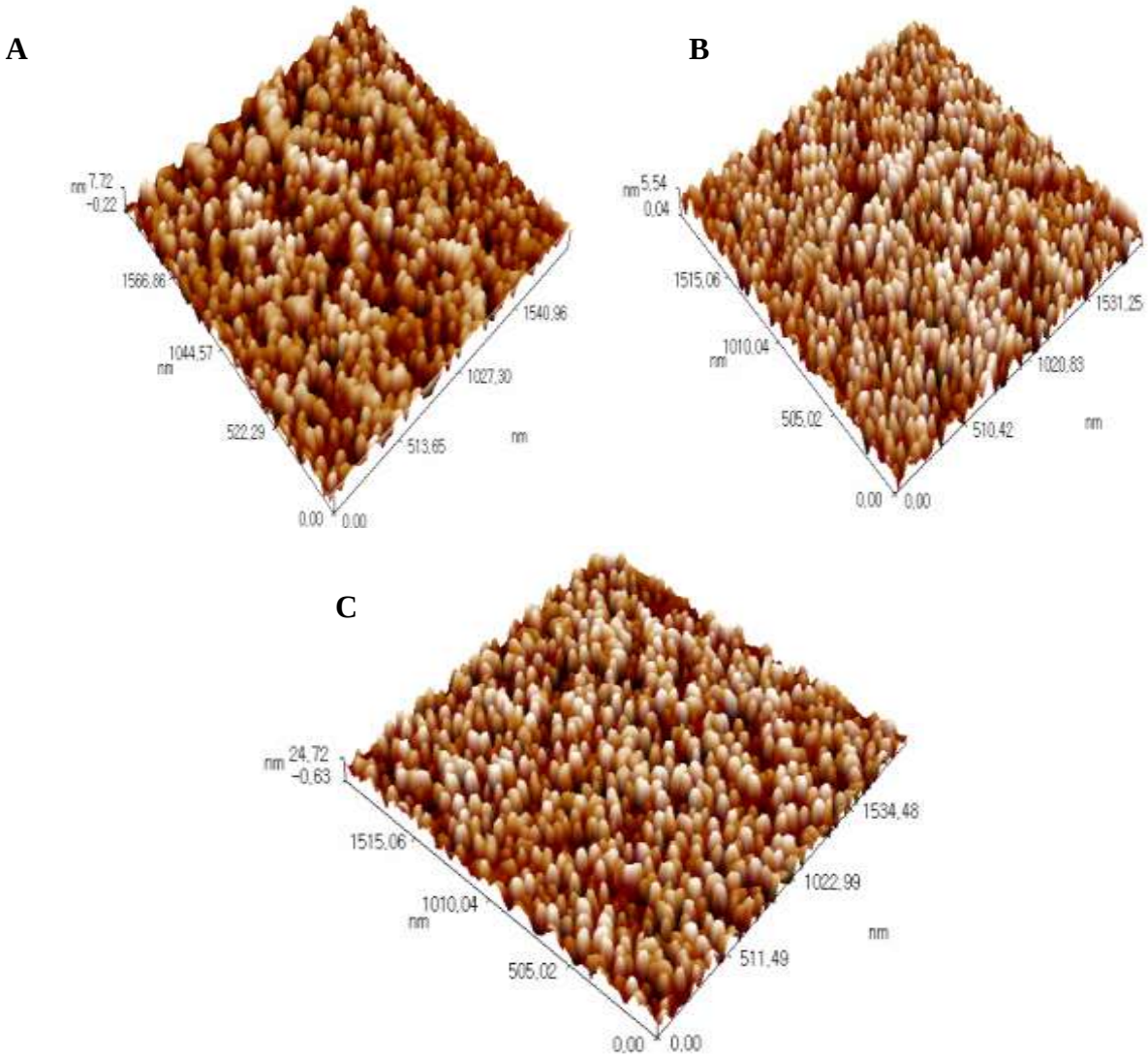

Figure 6- AFM images of ag nanoparticles prepared at different pulse laser energy A) 500mJ, B) 600mJ and C) 700mJ with magnetic field.

In addition, Table- 2 illustrated that the average roughness of Ag NPs film surface decreased with increasing pulse laser energy in the absence of magnetic field. This effect is due to the decrease in grain size with increasing pulse laser energy [16]. While in the presence of magnetic field, the average roughness of Ag NPs film surface was decreasing and then increasing with increasing pulse laser energy. This result implies that the grain size is changed with the change in pulse laser energy when the magnetic field is applied.

4.5 Fourier Transform Infrared Spectroscopy (FTIR)

Size distribution and characterization of the Ag nanoparticle synthesized by laser at the different laser energies with and without magnetic field were explored further using FTIR. Figure 7 shows the FTIR spectrum of Ag NPs prepared at different pulse energies (500, 600 and 700 mJ) in the absence of magnetic field. The spectrum shows a broad peak at 3421.48 to 3448.49 cm^{-1}in the high frequency area together with a sharp peak at 1635.52cm^{-1}, corresponding to the stretching and bending vibration of OH groups of water molecules [17,18]. The absorption peaks corresponding to 690 cm^{-1} are representing Ag-O deformation [19]. The peak that belongs to the vibration of the Ag-Ag metallic bonds cannot be seen in this graph because the FTIR used the mid-infrared ray (4000-400 cm^{-1}) that is not suitable to measure the vibration frequency of metal-metal bonds [20].

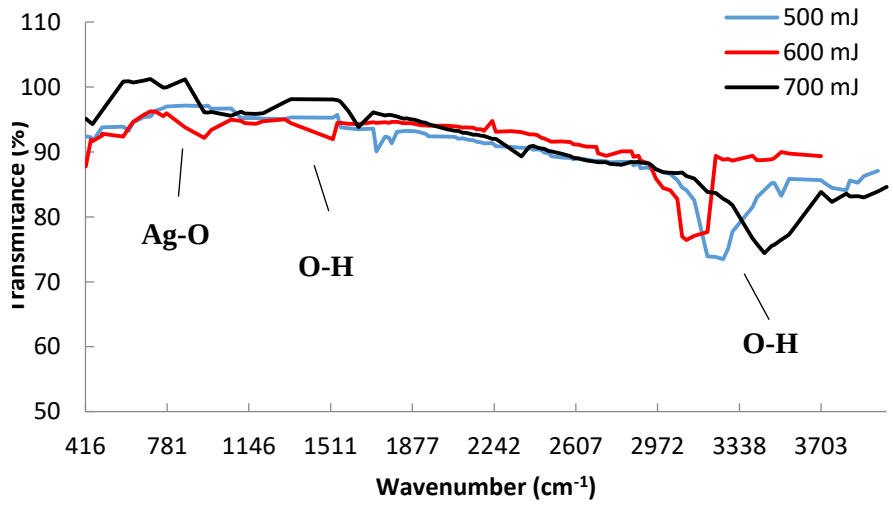

Figure 7-FTIR spectrum of Ag NPs prepared at different pulse energies without magnetic field.

When the laser energy increases, the FTIR spectrum shows that all absorption peaks are reduced and shifted, which depends on laser energy.
Figure-8 demonstrates the FTIR spectrum of AgNPs prepared at different pulse energies in the presence of the magnetic field.

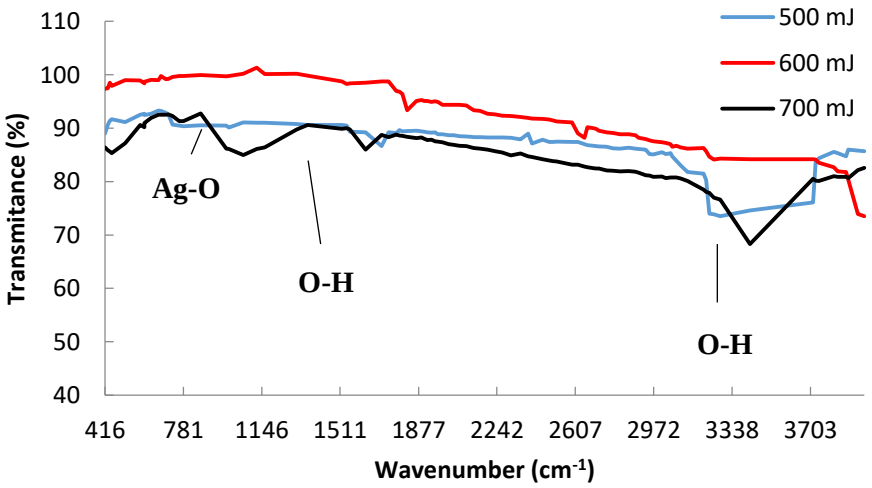

Figure 8-FTIR spectrum of Ag NPs prepared at different pulse energies in the presence of magnetic field.

Figure-8 shows the FTIR spectrum of Ag NPs prepared at different laser energies in the presence of magnetic field. The spectrum reveals absorption peaks at 3446.56, 3452.34 and 3450.41 cm^{-1} at laser energy of 500, 600, 700 mJ, respectively, together with one sharp peak at 1635.52 cm^{-1} which is attributed to the stretching and bending vibration of OH groups of water molecules [17,18]. One small absorption peaks at cm^{-1} corresponded to the Ag-O bond which appears when the pulse energy is equal to 500 and 600 mJ, and this peak disappeared when laser energy became 700 mJ. The spectrum shows that the absorption peaks in the spectrum were shifted toward smaller wavelengths when the laser energy increased from 500mJ to 600 mJ, . Then there was no shift in the absorption peak when the laser energy became 700 mJ, which could be due to agglomeration and the formation of larger

particles. Consequently, we can conclude that the AgNPs characteristics such as size and shape change with the changes in laser energy in the presence of magnetic field.

5. Conclusion

Preparation of silver NPs by the Q-switched Nd:YAG laser ablation method at different pulse laser energies in distilled water, in the presence and absence of the magnetic field, was investigated. The results show that Ag NPs in these experimental condition are almost spherical in shape. The number of Ag NPs was increased by increasing laser energy, while particle size of the Ag NPs was reduced by increasing laser energy without magnetic field. While, in the presence of magnetic field, Ag NPs size slightly increased by increasing the laser energy. The amount of Ag NPs was increased in the presence of magnetic field using the same laser energy. According to AFM results, the presence of magnetic field did affect the average diameter of Ag NPs. The presence of a magnetic field resulted in a change in grain size of Ag NPs with increasing laser energy. While, XRD data illustrated that the magnetic field caused an increase in the crystallite size of Ag NPs.

6. References

1. Xiao, J., Liu, P., Wang, C. and Yang, G. **2017**. External field-assisted laser ablation in liquid: An efficient strategy for nanocrystal synthesis and nanostructure assembly**,** *Progress in Materials Science*, **87**: 140–220.
2. Ganjalia, M., Ganjalib, M., Vahdatkhahc P. and Marashid, S. **2015**. Synthesis of Ni Nanoparticles by Pulsed Laser Ablation Method in Liquid Phase, *Procedia Materials Science*, **11**: 359 – 363.
3. Abbas, Q. **2019**. Effect of Target properties on the Plasma Characteristics that produced by Laser at Atmospheric Pressure, *Iraqi Journal of Science*, **60**(6): 1251-1258.
4. Humud, H. and Kadhem, S. **2015** . Laser-Induced Modification of Ag and Cu Metal Nanoparticles Formed by Exploding Wire Technique in Liquid, *Iraqi Journal of Science*, **56**(4B): 3135-3140.
5. Khan, M., Al-Marri, A., Khan, M., Rafi Shaik, M., Mohri, N., Farooq Adil, S., Kuniyil, M., Alkhathlan, H., Al-Warthan, A., Tremel, W., Nawaz Tahir, M. and Rafiq H Siddiqui, M. **2015**. Green Approach for the Effective Reduction of Graphene Oxide Using Salvadora persica L. Root (Miswak) Extract, *Nanoscale Research Letters*,**10**(281): 1-9.
6. Sasirekha, R., Mangayarkarasi, R., Ganesan, S. and Santhanam, P. **2018**. Biosynthesis, characterization antibacterial effects of silver nanoparticle by using Carica papaya fruit extract and it's interaction with an anticancer drug (5- fluorouracil)**,** *Journal of Innovations in Pharmaceutical and Biological Sciences (JIPBS)*, **5**(1): 01-07.
7. Roldán, M. V., Pellegri, N.S. and de Sanctis,O. A. **2012**. Optical response of silver nanoparticles stabilized by amines to LSPR based sensors, *Procedia Materials Science*,**1**: 594 – 600.
8. Anandalakshmi, K., Venugobal, J. and Ramasamy,V. **2016**. Characterization of silver nanoparticles by green synthesis method using Pedalium murex leaf extract and their antibacterial activity, *Appl Nanosci*, **6**: 399–408.
9. Haider M. J. and Mehdi, M. S. **2014**. Effect of Experimental Parameters on the Fabrication of Silver Nanoparticles by Laser Ablation, *Tech.Journal*, **32B**(4):704-709.
10. D. Malina, D., Sobczak-Kupiec, A., Wzorek, Z. and Kowalski, Z. **2012**. Silver Nanoparticles Synthesis with Different Concentrations of Polyvinylpyrrolidone, *Digest Journal of Nanomaterials and Biostructures*, **7**(4): 1527-1534.
11. Sportelli, M.C., Izzi, M., Volpe, A., Clemente, M., Picca, R. A., Ancona, A., Lugarà, P.M., Palazzo, G. and Cioffi, N. **2018**. The Pros and Cons of the Use of Laser Ablation Synthesis for the Production of Silver Nano-Antimicrobials**,** *Antibiotics*, **7**(67): 1-28.
12. S. B. Aziz, S. B., Abdullah, O. G., Saber, D. R., Rasheed, M. A., Ahmed, H. M. **2017**. Investigation of Metallic Silver Nanoparticles through UV-Vis and Optical Micrograph Techniques, *Int. J. Electrochem. Sci.*, **12**: 363 – 373.
13. D. Dorranian, D., Tajmir, S. and Khazanehfar, F. **2013**. Effect of Laser Fluence on the Characteristics of Ag Nanoparticles Produced by Laser Ablation, *Soft Nanoscience Letters*, **3**: 93-100.
14. Subha, V., Kirubanandan, S. and Renganathan, S. **2016**. Green Synthesis of Silver Nanoparticles from a Novel Medicinal Plant Source Roots Extract of Mukia maderaspatana, *Colloid and Surface Science*,**1**(1): 14-17.

15. Issa, B., B., Obaidat, I. M., Albiss, I.M. and Haik, Y. **2013**. Magnetic Nanoparticles: Surface Effects and Properties Related to Biomedicine Applications, *Int. J. Mol. Sci.*, **14** : 21266-21305.
16. Sanjeev, S. and Kekuda, D. **2015**. Effect of Annealing Temperature on the Structural and Optical Properties of Zinc Oxide (ZnO) Thin Films Prepared by Spin Coating Process, *Materials Science and Engineering*, **73**: 1-5.
17. Moosa, A. A. and Jaafar, J. N. **2017**. Green Reduction of Graphene Oxide Using Tea Leaves Extract with Applications to Lead Ions Removal from Water, *Nanoscience and Nanotechnology*, **7**(2): 38-47.
18. Pavoskia, G., Maraschinb, T., Fima, F. C., Balzarettid, N. M., Gallanda, G. B., Mourae, C. S. and Bassob,N. R. **2017**. Few Layer Reduced Graphene Oxide: Evaluation of the Best Experimental Conditions for Easy Production, *Materials Research*, **20**(1): 53-61.
19. Ghanipour, M. and Dorranian, D. **2013**. Effect of Ag-Nanoparticles Doped in Polyvinyl Alcohol on the Structural and Optical Properties of PVA Films, *Journal of Nanomaterials*, 1-10.
20. Gharibshahi, L., Saion, E., Gharibshahi, E. and Shaari, A. **2017**. Structural and Optical Properties of Ag Nanoparticles Synthesized by Thermal Treatment Method and Khamirul Amin Matori, *Materials*, **10**(402): 1-13.